Anomalous Evolution of Plasma Composition During a Small Solar Flare

Understanding the Strange Composition Evolution using Hinode/EIS, SDO/AIA, SDO/HMI; and Techniques like FIP Bias Measurements and Wavelet Analysis

Andy S.H. To
1st Year PhD Student
UCL / MSSL
shu.to.18@ucl.ac.uk

Collaborators: David M. Long, Deborah Baker, Lidia van Driel-Gesztelyi, Gherardo Valori, David H. Brooks,

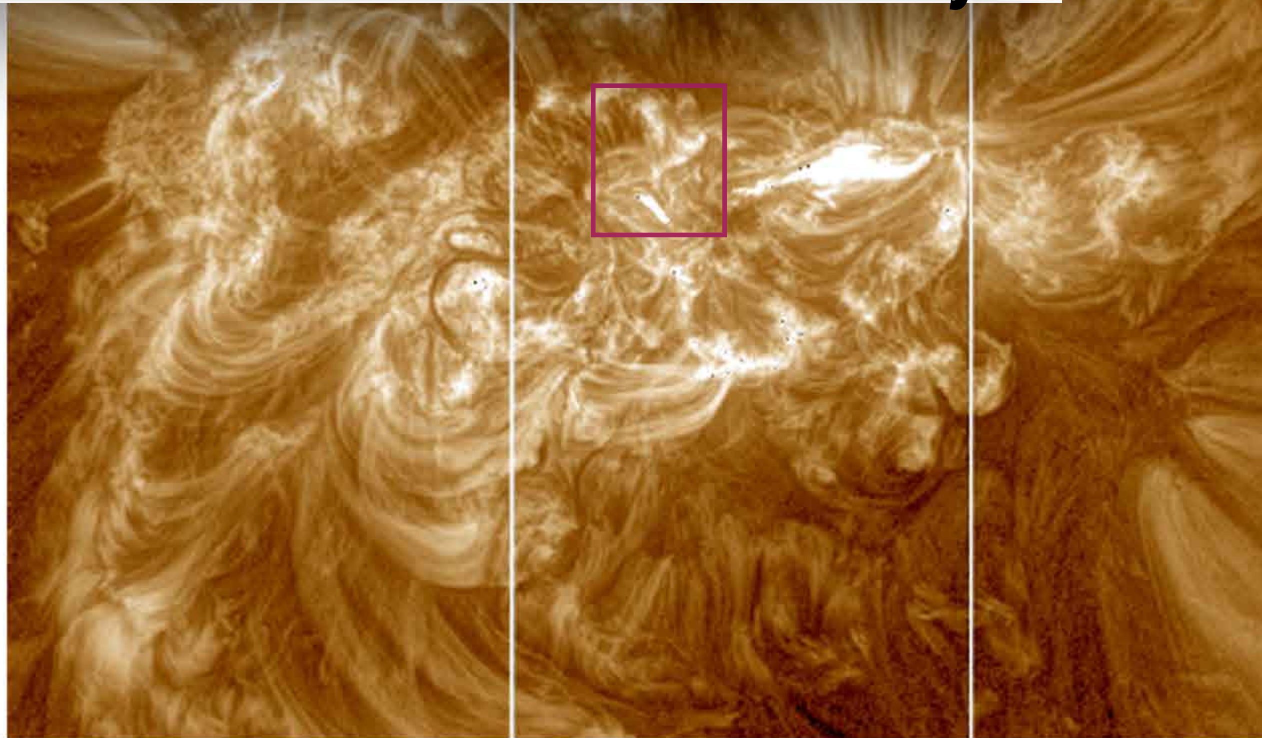

Why Composition & How Do We Measure It?

Sun's Photospheric Elemental Composition

Hydrogen	Helium	Metal
71.0%	27.1%	1.9%

6000+ Earth Masses!

Complex Processes

on the Sun lead to a variation in metal abundances in the corona, compared to the photosphere

UNEXPECTED because the corona originates from the photosphere

Unique Emission Lines of Metals

provide us with a tool to study metal abundances there, and gave us an insight into the processes in the solar atmosphere

Categorising Composition - First Ionisation Potential

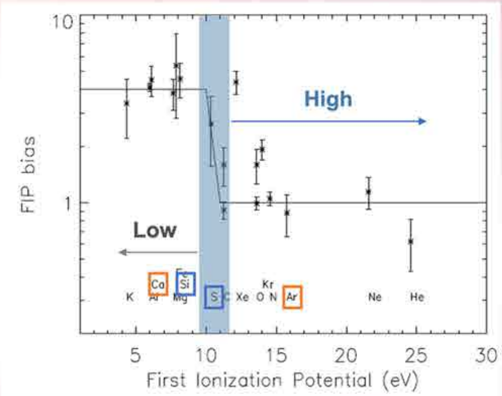

Method to Categorise Composition

First Ionisation Potential (FIP)

Low FIP elements (FIP < 10eV)	High FIP elements (FIP > 10eV)
e.g. Calcium, Silicon	e.g. Argon, Sulphur

High FIP and low FIP elements are separated by this sharp turn at 10eV, highlighted by the blue region. In a developed active region, the low-FIP elements are usually more abundant than the high-FIP ones, relative to their photospheric values. The ratio between their solar atmosphere abundances to their photospheric abundances is called the FIP bias. In this analysis, we use two pairs of emission lines, the ratio between low FIP silicon and high FIP sulphur highlighted in blue, and the ratio between low FIP calcium and high FIP argon highlighted in orange

General View of Today's Data

- AR 11967, > 32 Days of history, magnetically complex
- hosted 83 C-class flares, 28 M-class flares
- We study flares in between two big sunspots (S1 & S3, white box).

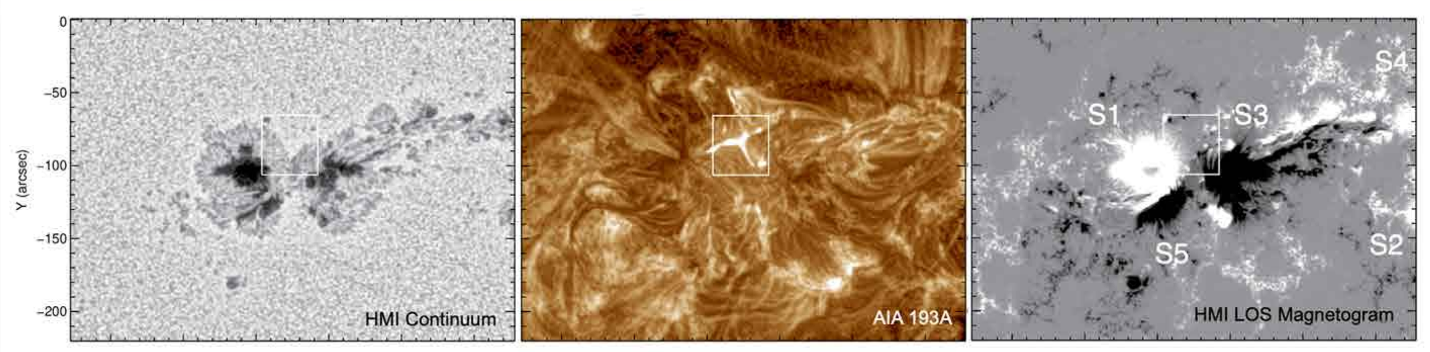

[1] Del Zanna, G., & Mason, H. E. (2014). Elemental abundances and temperatures of quiescent solar active region cores from x-ray observations. A&A, 565 A14.

[2] von Steiger, R., Geiss, J., & Gloeckler, G. (1997). Composition of the solar wind. cwh, 581.

UCL

shu.to.18@ucl.ac.uk

3 Flares in AR 11967 on 2 Feb 2014

09:31 UT

C class flare shown in the 193A image, and 94A light curve.

13:35 UT

Small flare, did not show up in GOES X-ray curve.

14:44 UT

Small flare, did not show up in GOES X-ray curve, but we caught this one in action while EIS was scanning. The timing of the EIS scans are indicated by the blue horizontal lines. This is the observation we are interested in.

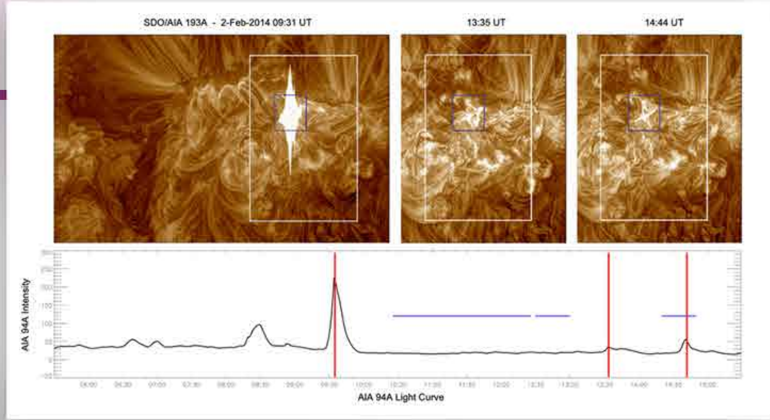

FIP Bias Evolution Using Two Pairs of Elements

Si X/S X composition map (~1.5MK)

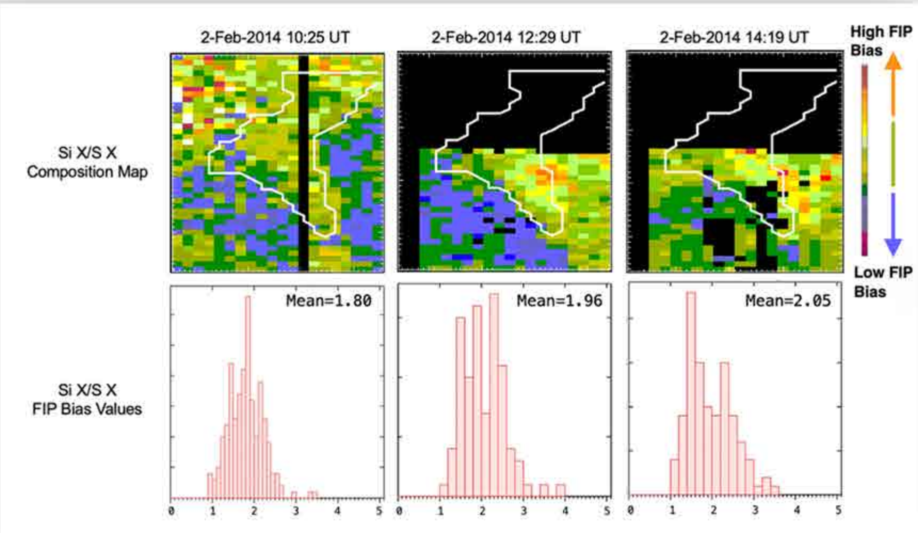

Si X/S X composition map, with white contour indicating the flaring region. Black region indicates pixels with a bad chi^2

Histogram indicates no change across the three rasters.

Ca XIV/Ar XIV composition map (~3.5MK)

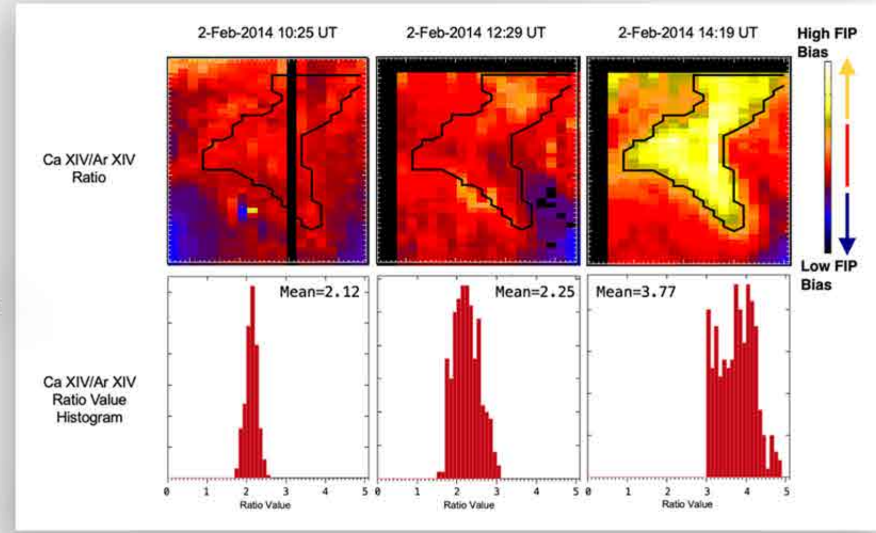

Ca XIV/Ar XIV composition map shows an increase of ~1.5 in FIP bias value in the raster which caught the flare!

UCL

shu.to.18@ucl.ac.uk

Further Investigation - Wavelet Analysis

Looking for wave signatures, we employed the wavelet analysis on AIA 94A, 131A, 304A, 1600A, 1700A and HMI continuum to our third flare, within the box we showed earlier.

Indeed, we found some evidence of waves present in the flare emission, while the sequence of time lags between the peak times in different passbands suggest that waves produced by the flare in the corona propagated through the transition region towards the chromosphere and upper photosphere, consistent with the interpretation of Fletcher and Hudson (ApJ, 2008). The wave may be either an Alfven wave, or something else excited by an Alfven wave from the flare, because all other flare generated wave modes would likely reflect or dissipate before reaching the low chromosphere.

This perhaps suggests that the Alfven waves that are crucial for the ponderomotive force model are present.

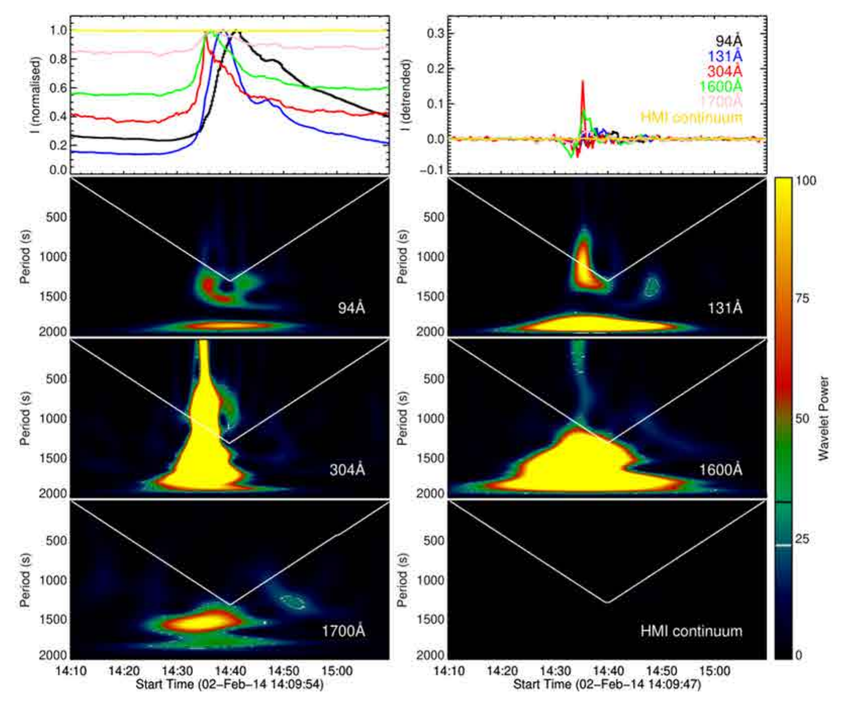

Conclusion - 2 Possible Physical Interpretations

1. Ablation During the Flare

Current fractionation models describe composition evolution of a near-time-independent structure, like active region and solar wind, and predict that fractionation (change in the elemental composition) occurs at the top of the chromosphere. Warren (2014) went one step further to suggest that in large flares (M and X class flares), the bulk of flare plasma is ablated from deep in the chromosphere, below where fractionations occur. However, this would likely lead to more photospheric abundances in both line pairs.

2. High-FIP Element Sulphur Behaves like a Low-FIP Element

The relatively constant Si/S ratio compared with the strongly increasing Ca/Ar ratio suggests that the high-FIP S is behaving more like a low-FIP than a high-FIP element. It can do this if fractionation occurs in the low chromosphere, where the background gas is neutral H. Our wavelet analysis suggests that this is what is happening. In the strong chromospheric magnetic field between two large spots, where this flare is taking place, the fractionation height of S shifts to the low chromosphere making it behave more like a low-FIP element (Laming et al. 2019). Both Si and S fractionate in this flare and the Si/S ratio does not change, while the noble gas (high-FIP) Ar maintains its high-FIP behaviour and we see strong increase in the Ca/Ar ratio.

[3] Fletcher, L., & Hudson, H. S. (2008). Impulsive Phase Flare Energy Transport by Large-Scale Alfvén Waves and the Electron Acceleration Problem. Astrophys. J., 675(2), 1645–1655.

[4] Laming, J. M. (2015). The FIP and Inverse FIP Effects in Solar and Stellar Coronae. Living Rev. Sol. Phys., 12(1), 2–76.

[5] Warren, H. P. (2014). Measurement of Absolute Abundances in Solar Flares. Astrophys. J. Lett., 786(1), L2.

[6] Laming, J. M., Vourlidas, A., Korendyke, C., Chua, D., Cranmer, S. R., Ko, Y.-K., ...Wood, B. E. (2019). Element Abundances: A New Diagnostic for the Solar Wind. Astrophys. J., 879(2), 124.

UCL

shu.to.18@ucl.ac.uk